

Space-and-time-synchronized simultaneous vehicle tracking/formation using cascaded prescribed-time control

Peng Wang^a, Ziyin Chen^b, Xiaobing Zhang^{a,*}

^a*School of Energy and Power Engineering, Nanjing University of Science and Technology, Nanjing 210094, China*

^b*Beijing Institute of Space Mechanics and Electricity, China Academy of Space Technology, Beijing 100093, China*

Abstract

In this paper, we present a space-and-time-synchronized control method with application to the simultaneous tracking/formation. In the framework of polar coordinates, through correlating and decoupling the reference/actual kinematics between the self vehicle and target, time and space are separated, controlled independently. As such, the specified state can be achieved at the predetermined terminal time, meanwhile, the relative trajectory in space is independent of time. In addition, for the stabilization before the predesigned time, a cascaded prescribed-time control theorem is provided as the preliminary of vehicle tracking control. The obtained results can be directly extended to the simultaneous tracking/formation of multiple vehicles. Finally, numerical examples are provided to verify the effectiveness and superiority of the proposed scheme.

Keywords: Synchronization of space and time, cascaded prescribed-time control, simultaneous arrival

1. Introduction

In practice, positioning and tracking problems are of special interest to many important applications which involve the trajectory/path following of autonomous vehicles [1, 2], formation/containment control of multiple autonomous vehicles [3, 4] and so on. It is noted that there exist two important scales in positioning and tracking: space and time. Existing researches usually focus on when to reach a designated location, or what kind of trajectory in space, but few considerations involve both of them at the same time, which inspires this work.

First of all, a concept named 'synchronization of space and time' is proposed.

Synchronization of space and time: We summarize the following three characteristics for the synchronization of space and time:

- (i) Time and space are separated and can be controlled independently;
- (ii) In the time control, the specified position can be reached at the predetermined instant;

- (iii) In the space control, the trajectory in space is independent of time, that is, the trajectory in space is fixed regardless of the terminal time.

In the following, two aspects are discussed.

Prescribed-time/distance control: Finite/fixed/prescribed-time control has drawn increasing attention in recent years in view of the fact that many practical applications require severe time response constraints. Homogeneity property gives a useful analysis for HOSM (high-order sliding mode) control, and if an asymptotically stable system is homogeneous of a negative degree, then it is finite-time stable to a sliding manifold (see [5–7]). However, the settling time in these finite-time methods grows unbounded when initial conditions tend to infinity, and the initial conditions are hard to acquire in some practical situations [8]. Fixed-time stability requires a controller (observer) to provide some desired control (observation) precision at a given time, independent of the initial conditions, and the settling time is subject to an upper bound but varies due to uncertainties and nonlinearities [9, 10]. The reviews upon the fixed-time stability and its applications can be found in [11]. However, the fixed-time settling time can not be preassigned arbitrarily since its upper bound is subject to certain restrictions [12]. Moreover, prescribed-time control employs a scaling of state by a function of time that grows unbounded to the

*Corresponding author

Email addresses: benjywp711@gmail.com (Peng Wang),
chenziyin_heu@163.com (Ziyin Chen),
zhangxb680504@163.com (Xiaobing Zhang)

terminal time and yields the regulation in prescribed finite time (see [13, 14]). Furthermore, regarding the prescribed-distance control problem, the system regulation can be achieved before the prescribed distance is reached. The conversion between the prescribed-distance control and the existing prescribed-time control only requires the distance-driven transformation for the differential dynamic system model, which will be answered in this paper.

Simultaneity in time: The finite-time distributed consensus has been a popular topic in recent years, which is known as one of the most important issues in cooperative control [14–16]. However, for some classes of practical systems, this finite-time convergence is not enough operating, for example, for a service robot hand, its joints are usually required to reach the desired angle at the same time; the proximity operations require that the pursuer perform the translational and rotational maneuvers with respect to the target simultaneously [17]; for the multi-missile interception active defense [18, 19], multiple missiles are expected to strike the target simultaneously. In this regard, simultaneity in time for multi-agent systems are of great importance. The works in [20, 21] proposed the time-synchronized consensus control, focusing on how to design a controller which drives all the elements of all the agent states to consensus at the same time; and fixed-time-synchronized consensus, where the upper bound of the synchronized settling time is independent of the initial states of multi-agent systems.

Contributions of this work: The main contributions are stated as following

- (i) In the framework of polar coordinates, given a reference relative trajectory, the developed distance-driven controller enables the prescribed-distance stability and achieves the separation between space and time. In comparison, few of the existing works consider the distance-driven transformation about the tracking problem. Moreover, the work in [19] employs a different distance-driven transformation and obtains the travelling range in advance, while the velocity value is set fixed and the target is assumed stationary;
- (ii) Through correlating and decoupling the reference/actual kinematics between the self vehicle and target, the control variables related to velocity and inclination angle are controlled respectively to form synchronization between the arrival time and path trajectory. This kind of correlating and decoupling operations give the freedom to the velocity control in polar coordinates, which is proposed for the first time, to the best of the authors' knowl-

edge;

- (iii) A cascaded prescribed-time control theorem is proposed which enables the prescribed-time stabilization for the general strict-feedback systems. Compared with the prescribed-time control [13, 14], the proposed theorem eliminates restrictions on the system model and allows the uncertainties and the remaining-time-related interconnections in each subsystem; the cascaded prescribed-time tracking problem can be directly solved through the separately prescribed-time control design of each subsystem;
- (iv) The synchronization of space and time control enables the simultaneous arrival of multiple vehicles which reach the designated position or achieve formation simultaneously. Compared with the existing simultaneous control work, the target in the simultaneous tracking/formation problem does not have to be set stationary as in [18, 19], and the simultaneous property can be directly derived from the proposed space-and-time-synchronized control.

Notation: Throughout this paper, \mathcal{R} denotes the set of real numbers, $\mathcal{R}^{n \times m}$ represents the set of $n \times m$ real matrix, \mathcal{N}_+ is the set of positive integers. $(\cdot)^T$ is the transpose of one matrix, $\text{diag}(\cdot)$ represents the diagonal matrix. $|\cdot|$ is the absolute value of a scalar and $\|\cdot\|$ is defined as the Euclidean norm of a vector. Given a matrix M , $M > 0$ (or $M < 0$) means that M is a positive definite (or negative definite) matrix, $\lambda_{\min}(M)$ and $\lambda_{\max}(M)$ denote the the minimum and maximum eigenvalue of matrix M , respectively.

2. Formulation of space-and-time-synchronized problem

As the geometry of planer scenario depicted in Fig. 1, the subscripts s and t denote the self vehicle and target, respectively, the subscripts 0 and f represent the initial time and the predetermined time, respectively. $R \in \mathcal{R}$ represents their relative distance along the line of sight (LOS) angle $q \in \mathcal{R}$. $V_s \in \mathcal{R}$ and $V_t \in \mathcal{R}$ denote the velocities of the vehicle and target, respectively, $\theta_s \in \mathcal{R}$ and $\theta_t \in \mathcal{R}$ are their corresponding path angles, $\eta_s \in \mathcal{R}$ and $\eta_t \in \mathcal{R}$ represent the heading angles. The tracking kinematics between the vehicle and target in the framework of polar coordinates are modeled as

$$\begin{aligned} \dot{R} &= -V_s \cos \eta_s + V_t \cos \eta_t, \\ R\dot{q} &= V_s \sin \eta_s - V_t \sin \eta_t, \\ \eta_s &= q - \theta_s, \quad \eta_t = q - \theta_t \end{aligned} \quad (1)$$

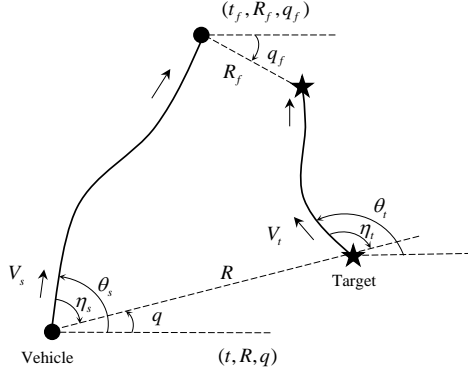


Figure 1: Geometry description

with the initial condition $R(0) = R_0$, $q(0) = q_0$, $\eta_s(0) = \eta_{s0}$ and $V_s(0) = V_{s0}$. When it comes to a special case $V_t = 0$ which means a stationary target point, the kinematics model (1) is reduced to a positioning problem.

Define the pair (t, R, q) : at time t , the distance and LOS angle between the vehicle and target are R and q , respectively. We can now formulate the problem as follows:

Problem 1. (Synchronization of space and time) For a vehicle tracking problem (1), how to ensure the vehicle starting from (t_0, R_0, q_0) eventually realizes (t_f, R_f, q_f) and gets maintained in (t, R_f, q_f) for $t > t_f$?

Algorithm 1. For the sake of generality, the solution with respect to Problem 1 can be summarized as

- (i) In the framework of polar coordinates, introduce the reference trajectory (R_d, q_d) for the vehicle-target relative motion, which achieves the separation of time and space, see Section II.A;
- (ii) Correlate and decouple the reference/actual relative kinematics to obtain the separated control variables related to velocity V_s and inclination angle η_s , see Section II.B;
- (iii) The travelling time and path trajectory are controlled respectively to form synchronization between space and time.

2.1. Reference relative tracking trajectory

The motion equations for the reference tracking problem are given by

$$\begin{aligned} \dot{R}_d &= -V_d \cos \eta_d, \\ R_d \dot{q}_d &= V_d \sin \eta_d \end{aligned} \quad (2)$$

where R_d and q_d denote the distance and LOS angle of the reference trajectory, respectively, V_d and η_d are the

corresponding velocity and heading angle, respectively. Their initial conditions are set $R_d(0) = R_0$, $q_d(0) = q_0$, $\eta_d(0) = \eta_{d0}$ and $V_d(0) = V_{d0}$.

Define a new distance-scaled variable r_d and a prescribed value r_f

$$\begin{aligned} r_d &= \ln(R_0 - R_{f1}) - \ln(R_d(t) - R_{f1}), \quad R_d \in (R_f, R_0], \\ r_f &= \ln(R_0 - R_{f1}) \end{aligned} \quad (3)$$

where $R_{f1} = R_f - 1$. It is obvious that $r_d = r_f$ when $R_d = R_f$. The relationship between the distance-scaled variable r_d and the actual time t is subject to

$$\dot{r}_d = V_d \cos \eta_d / (R_d - R_{f1}), \quad R_d \in (R_f, R_0]. \quad (4)$$

Taking derivative with respect to the distance-scaled variable r_d , rather than the time variable t , yields the rewritten dynamics: when $r_d \in [0, r_f)$,

$$\begin{aligned} \frac{dq_d}{dr_d} &= \frac{R_d - R_{f1}}{R_d} \tan \eta_d, \\ \frac{d^2 q_d}{dr_d^2} &= \frac{R_d - R_{f1}}{V_d \cos \eta_d} \left[\frac{R_d - R_{f1}}{R_d \cos^2 \eta_d} \frac{d\eta_d}{dt} - \frac{R_{f1} V_d \sin \eta_d}{R_d^2} \right]. \end{aligned} \quad (5)$$

Theorem 1. Consider the system in form of (2).

(i) When $R_d \in [0, r_f)$, the control law of η_d is designed according to (6). The system state pair (q_d, η_d) asymptotically converges to the desired value $(q_f, 0)$ before r_d approaching the prescribed value r_f .

$$\begin{aligned} \dot{\eta}_d &= -\frac{R_d V_d \cos^3 \eta_d}{(R_d - R_{f1})^2} \left[\frac{k_{d2}}{r_f - r_d} \frac{dq_d}{dr_d} + \frac{k_{d1}(q_d - q_f)}{(r_f - r_d)^2} \right] \\ &\quad + \frac{R_{f1} V_d \cos^2 \eta_d \sin \eta_d}{(R_d - R_{f1}) R_d}. \end{aligned} \quad (6)$$

When letting $k_{d1} = N_1 N_2$, $k_{d2} = N_1 + N_2 - 1$, $N_1 < N_2$ and $N_1, N_2 \in \mathcal{N}_+$, the travel range can be calculated as

$$S_d = \int_{R_f}^{R_0} \sqrt{1 + (\tan \eta_d)^2} dR_d. \quad (7)$$

In this sequel, S_d is irrespective of V_d , the travel time t_f is only related to the velocity V_d . For any constant velocity V_d , the travel time is $t_f = S_d / V_d$.

(ii) When R_d approaches R_f , through $\dot{V}_d = 0$ and $\dot{\eta}_d = 0$, the system state pair (R_d, q_d, η_d) gets maintained in the desired value $(R_f, q_f, 0)$.

Proof. See Appendix A. \square

Remark 1. Here comes the motivation of introducing the proposed distance-scaled variable r and doing the r -related dynamics transformation:

- (i) The system dynamics (5) with respect to the introduced distance-scaled variable r_d is independent of time and directly linked to the terminal distance R_f . As a result, this proposed distance-related transformation is more intuitive to the distance tracking problem like the prescribed-distance control;
- (ii) This kind of transformation (3) together with the controller (6) enables the achievement of regulation objective before $r_d = r_f$. The resultant irrelevance between S_d and V_d creates a separation between space and time, which provides the possibility for the space-and-time-synchronized control;
- (iii) Such a state transformation brings η_d into a state-related form, i.e. $\tan \eta_d = \frac{dq_d}{dr_d} \frac{R_d}{R_d - R_f}$, such that the specific expression η_d in space can be directly obtained in (36). Some heading-angle-constrained problems can be handled through appropriate parameter selection when considering the field-of-view limits.

2.2. Kinematic modelling

To correlate the reference/actual relative kinematics, we define the following error variables, i.e., distance error $R_e = R - R_d$, LOS angle error $q_e = q - q_d$, angle $\eta_e = \eta_s - \eta_d$, velocity error $V_e = V_s - V_d$.

Taking time derivative of R_e along the solutions of (1) and (2) leads to

$$\begin{aligned} \dot{R}_e &= -V_s \cos \eta_s + V_s \cos \eta_d - V_s \cos \eta_d \\ &\quad + V_d \cos \eta_d + V_t \cos \eta_t \\ &= -V_s (\cos(\eta_d + \eta_e) - \cos \eta_d) - V_e \cos \eta_d + V_t \cos \eta_t \\ &= -V_e \cos \eta_d + V_t \cos \eta_t \\ &\quad + V_s \left[\cos \eta_d \frac{1 - \cos \eta_e}{\eta_e} + \sin \eta_d \frac{\sin \eta_e}{\eta_e} \right] \eta_e. \end{aligned} \quad (8)$$

A similar operation for q_e brings

$$\begin{aligned} \dot{R}q_e &= V_s \sin \eta_s - V_s \sin \eta_d + V_s \sin \eta_d - V_d \sin \eta_d \\ &\quad - V_d \sin \eta_d (R_e/R_d) - V_t \sin \eta_t \\ &= V_e \sin \eta_d + V_s \left[\sin \eta_d \frac{\cos \eta_e - 1}{\eta_e} + \cos \eta_d \frac{\sin \eta_e}{\eta_e} \right] \eta_e \\ &\quad - V_d \sin \eta_d (R_e/R_d) - V_t \sin \eta_t. \end{aligned} \quad (9)$$

Invoking the fact

$$\frac{1 - \cos \eta_e}{\eta_e} = \int_0^1 \sin(\tau \eta_e) d\tau, \quad \frac{\sin \eta_e}{\eta_e} = \int_0^1 \cos(\tau \eta_e) d\tau \quad (10)$$

and combing the above dynamics of R_e and q_e , we readily obtain the kinematic model of vehicle tracking problem

$$\begin{bmatrix} \dot{R}_e \\ R\dot{q}_e \end{bmatrix} = M(\eta_s, \eta_e, V_s) \begin{bmatrix} V_e \\ \eta_e \end{bmatrix} + G(R_e, R_d, V_t, \eta_t, V_d, \eta_d) \quad (11)$$

where the detailed expressions of $M(\eta_s, \eta_e, V_s)$ and $G(R_e, R_d, V_t, \eta_t, V_d, \eta_d)$ are at the top of next page.

Remark 2. With regard to (10), a special case is when $\eta_e = 0$, through the L'Hospital rule and limit of indeterminate form, one obtains $(1 - \cos \eta_e)/\eta_e = 0$ and $\sin \eta_e/\eta_e = 1$.

Remark 3. As for the parameter matrix $M(\eta_s, \eta_e, V_s)$, its determinant is $|M(\eta_s, \eta_e, V_s)| = -V_s (\sin \eta_e/\eta_e) < 0$, which contributes to the full rank of $M(\eta_s, \eta_e, V_s)$ and enables the later matrix inversion operation.

2.3. Dynamic modelling

Define the control variable $u = [u_V \quad u_\theta]^T$ where u_V is the tangential acceleration and u_θ is the lateral acceleration. The vehicle's dynamic model is expressed by

$$\begin{aligned} \dot{V}_s &= u_V + d_V, \\ \dot{\theta}_s &= u_\theta/V_s + d_\theta \end{aligned} \quad (12)$$

where d_V and d_θ are the external disturbances.

As such, the compact system model combing (11) and (12) is written as

$$\begin{bmatrix} \dot{R}_e \\ \dot{q}_e \end{bmatrix} = \bar{M} \begin{bmatrix} V_s \\ \eta_s \end{bmatrix} - \bar{M} \begin{bmatrix} V_d \\ \eta_d \end{bmatrix} + \bar{G}, \quad (13a)$$

$$\begin{bmatrix} \dot{V}_s \\ \dot{\eta}_s \end{bmatrix} = B \begin{bmatrix} u_V \\ u_\theta \end{bmatrix} + H + F \quad (13b)$$

where $\bar{M}(R, \eta_s, \eta_e, V_s) = \text{diag}(1, 1/R)M$, $\bar{G}(R, R_e, R_d, V_t, \eta_t, V_d, \eta_d) = \text{diag}(1, 1/R)G$, $B(V_s) = \text{diag}(1, -1/V_s)$, $H(\dot{q}, \dot{R}, R, \eta_s) = [0 \quad \dot{q}]^T$, $F(d_V, d_\theta) = [d_V \quad -d_\theta]^T$.

3. Prescribed-time Control Design

For the prescribed-time control design, we reach the following consensus: as long as R_e and q_e converge to 0 before the final time t_f (before R converges to R_f), the vehicle (R, q) reaches the specified state (R_f, q_f) at the time t_f .

Problem 2. (Prescribed-time stabilization) For some kind of strict feedback systems like system (13a)(13b), how to ensure the system stability within the prescribed time $t \in [0, t_f]$?

$$M = \begin{bmatrix} -\cos \eta_d & V_s \left(\cos \eta_d \int_0^1 \sin(\tau \eta_e) d\tau + \sin \eta_d \int_0^1 \cos(\tau \eta_e) d\tau \right) \\ \sin \eta_d & V_s \left(\cos \eta_d \int_0^1 \cos(\tau \eta_e) d\tau - \sin \eta_d \int_0^1 \sin(\tau \eta_e) d\tau \right) \end{bmatrix}, \quad G = \begin{bmatrix} V_t \cos \eta_t \\ -V_t \sin \eta_t - V_d \sin \eta_d (R_e/R_d) \end{bmatrix}.$$

Algorithm 2. The corresponding solution with respect to Problem 2 is summarized as

- (i) The prescribed-time stability of a single first-order system can be achieved by employing a scaling of the state by a function of $t_f - t$;
- (ii) During the backstepping design procedure, the above first-order prescribed-time control design is repeated for each subsystem. In this sequel, a cascaded system consisting of two prescribed-time stable subsystems is obtained;
- (iii) The prescribed-time stability of the cascaded system is addressed and extended to cascade cases of multiple subsystems.

3.1. Prescribed-time stabilization of cascaded systems

Before processing the prescribed-time control, a cascaded prescribed-time theorem is presented as a preliminary. Cascades-based control essentially uses the designed control law to make the closed-loop system in a cascaded structure, which usually has the advantage of reducing the complexity of the controller and the difficulty of stability analysis.

Consider a kind of cascaded system described by

$$\begin{aligned} \Sigma_i : \dot{x}_i(t) &= f_i(t, x_i, \Delta_{x,i}) + g_i(t, x_i, x_{i+1})x_{i+1}, \\ \Sigma_n : \dot{x}_n(t) &= f_n(t, x_n, \Delta_{x,n}), i = 1, \dots, n-1 \end{aligned} \quad (14)$$

where $x_i(t) \in \mathcal{R}^{n_i}$ is the system state of subsystem Σ_i . $f_i(t, x_i, \Delta_{x,i})$, $g_i(t, x_i, x_{i+1})$ are continuous in their arguments, and locally Lipschitz in x_i , (x_i, x_{i+1}) respectively. For a simplified presentation, we view the cascaded system as the subsystem $\hat{\Sigma}_i$ perturbed by the output of subsystem Σ_{i+1} .

$$\hat{\Sigma}_i : \dot{x}_i(t) = f_i(t, x_i, \Delta_{x,i}). \quad (15)$$

Definition 1. [22] A continuous function $\alpha : [0, a) \rightarrow [0, \infty)$ belongs to class \mathcal{K} if it is increasing and $\alpha(0) = 0$, if moreover $\alpha(a) \rightarrow \infty$ as $a \rightarrow \infty$, it belongs to class \mathcal{K}_∞ . A continuous function $\beta : [0, a) \rightarrow [0, \infty)$ belongs to class \mathcal{L} if it is decreasing and $\beta(s) \rightarrow 0$ as $s \rightarrow \infty$. Again, a continuous function $\gamma : [0, a) \times [0, a) \rightarrow [0, \infty)$ belongs to class \mathcal{KL} if the mapping $\gamma(r, s)$ belongs to class \mathcal{K} with respect to r when fixed s , and the mapping $\gamma(r, s)$ decreases along s , i.e., $\gamma(r, s) \rightarrow 0$ as $s \rightarrow \infty$, when fixed r .

Definition 2. Consider the system $\dot{x} = f(t, x)$, where $f(t, x)$ is piecewise continuous in t and locally Lipschitz in x . The system is globally uniformly prescribed-time stable (GUPTS), if there exist a class \mathcal{KL} function $\gamma(\cdot, \cdot)$ and a settling-time t_f such that for any initial values $x(t_0)$:

$$\|x(t)\| \leq \gamma(\|x(t_0)\|, \tau(t, t_f)), \quad t_0 \leq t < t_f \quad (16)$$

where $\tau(t, t_f) \rightarrow \infty$ as $t \rightarrow t_f$, from which one obtains the strictly prescribed-time convergence of x : $x(t) \rightarrow 0$ as $t \rightarrow t_f$.

Theorem 2. Consider the cascaded system (14) with n subsystems. The globally uniformly prescribed-time stability (GUPTS) of the subsystem Σ_i , $i = 1, \dots, n$ can be obtained, if the following assumptions hold:

(i) Assumption on subsystem $\hat{\Sigma}_i$, $i = 1, \dots, n$: the subsystem $\hat{\Sigma}_i$ is GUPTS, and there exists a continuously differentiable Lyapunov function $V_i(t, x_i)$ such that

$$\begin{aligned} \alpha_{i1}(\tau)\|x_i\|^2 &\leq V_i(t, x_i) \leq \alpha_{i2}(\tau)\|x_i\|^2, \\ \dot{V}_i &= \partial V_i / \partial t + (\partial V_i / \partial x_i) f_i(t, x_i, \Delta_{x,i}) \\ &\leq -\alpha_{i3}(\tau)\|x_i\|^2 + b_i(\alpha_{i4}^2(\tau) / \alpha_{i3}(\tau)) \|\Delta_{x,i}\|^2, \\ \|\partial V_i / \partial x_i\| &\leq \alpha_{i4}(\tau) \|x_i\|, \\ \alpha_{i3}(\tau) &= \alpha_{i4}(\tau) \times \alpha_{i5}(\tau) \end{aligned} \quad (17)$$

where $\alpha_{ij}(\cdot)$, $j = 1, \dots, 5$ are class \mathcal{K}_∞ functions, $b_i > 0$.

(ii) Assumption on interconnection $g_i(t, x_i, x_{i+1})$, $i = 1, \dots, n-1$: there exist a class \mathcal{K}_∞ function $\alpha_{i6}(\cdot)$ and a positive constant $c_{g,i}$ satisfying

$$\begin{aligned} \|(\partial V_i / \partial x_i) g_i(t, x_i, x_{i+1})\| &\leq \alpha_{i6}(\tau) c_{g,i} \|x_i\|, \\ \lim_{t \rightarrow t_f} \alpha_{i6}(\tau) / (\alpha_{i3}(\tau) \alpha_{i+1,5}(\tau)) &= 0. \end{aligned} \quad (18)$$

Proof. See Appendix B. \square

Here we give an example which has been introduced in [13] for justification of assumption (17). Consider the first-order system governed by $\dot{x} = b(x, t)u + f(x, t)$ where $x, u \in \mathcal{R}$ and $0 < \underline{b} \leq |b(x, t)|$, $|f(x, t)| \leq d(t)\psi(x)$. Employing the residual-time-based scaling function $\mu(t-t_0) = \frac{T^{1+m}}{(T+t_0-t)^{1+m}}$, $t \in [t_0, t_0+T)$ with positive integer m , the controller was derived $u = -\frac{1}{\underline{b}}(k + \lambda\psi(x))^2 + \frac{1+m}{T}\mu(t-t_0)x$ with $k, \lambda > 0$. Following the Lyapunov function candidate $V = \omega^2/2$, $\omega = \mu(t-t_0)x$ and the presentation in [13], upon applying the control law, one

obtains $\dot{V} \leq -2k\mu V + \frac{\mu}{4\lambda} d^2$. In accordance with the proposed assumption, it is obvious $\alpha_{i1}(\tau) = a_1\mu^2 (0 < a_1 < 0.5)$, $\alpha_{i2}(\tau) = a_2\mu^2 (a_2 > 0.5)$, $\alpha_{i3}(\tau) = k\mu^3$, $\alpha_{i4}(\tau) = \mu^2$, $\alpha_{i5}(\tau) = k\mu$, $\alpha_{i6}(\tau) = \mu$, $b_i = 1/(4\lambda)$, all of which satisfy the condition in the applied assumption.

Remark 4. A strict feedback form of the cascaded system (14) can be obtained through the backstepping procedure

$$\begin{aligned} \Sigma_i : \dot{x}_i(t) &= -k_i(\tau)x_i + g_i(t, x_i, x_{i+1})x_{i+1} + \Delta_{x_i}, \\ \Sigma_n : \dot{x}_n(t) &= -k_n(\tau)x_n + \Delta_{x_n}, i = 1, \dots, n-1 \end{aligned} \quad (19)$$

where $k_i(\cdot)$, $i = 1, \dots, n$ are class \mathcal{K}_∞ functions. In principle, each subsystem can achieve the prescribed-time convergence due to the high-gain nature of $k_i(\tau)$ at the prescribed time t_f . Under the premise of (18), since the convergence of Σ_i is influenced by $\alpha_{i4}\|x_i\|\|x_{i+1}\|$ or $\alpha_{i4}\|x_i\|^2\|x_{i+1}\|$, an ideal manner would be for x_{i+1} to converge to zero before α_{i4} approaches infinity, which inspires the design $k_{i+1}(\tau) > k_i(\tau)$.

Remark 5. In the high-order prescribed-time control proposed in [13], the system model is in a standard integral form which limits that no uncertainties occur in the x_i 's dynamics. The reason lies in the repeated differentiation of the time-scaling transformation $\mu(t)x_1$ where $\mu(t)$ is a time-varying function which goes to infinity when t approaches t_f , as the form. However, the proposed cascaded prescribed-time control scheme in Theorem 2 has the distinguished features:

- (i) Eliminate restrictions on the system model, and allow the uncertainties in x_i ' dynamics;
- (ii) Allow the remaining-time $(t_f - t)$ -related interconnection $g_i(t, x_i, x_{i+1})$ appear in x_i ' dynamics;
- (iii) Each subsystem can also be individually designed for its prescribed-time stability performance.

3.2. Prescribed-time Controller design

For the sake of clarity, the following prescribed-time control design borrows from the techniques of backstepping and the overall dynamics are organized into a cascaded form. Invoking the definition of $\tau(t, t_f)$ in Definition 2, let a user-defined $\tau(t, t_f)$ satisfy $\tau(0, t_f) = 1$. Introduce now a time-varying scaling function of $t_f - t$ with $h > 0$

$$\mu(t, h) = \begin{cases} \tau^h(t, t_f), & t \in [0, t_f) \\ 1, & t \in [t_f, \infty) \end{cases} \quad (20)$$

whose derivative with respect to t yields

$$\begin{aligned} \dot{\mu}(t, h) &= \begin{cases} h\mu(t, h)(\dot{\tau}/\tau), & t \in [0, t_f) \\ 0, & t \in [t_f, \infty) \end{cases} \\ \dot{\tau}(t, t_f) &= 0, \quad t \in [t_f, \infty) \end{aligned} \quad (21)$$

For simplicity, define $\mu_1(t) = \mu(t, h_1)$, $\mu_2(t) = \mu(t, h_2)$ with $h_1, h_2 > 0$.

Theorem 3. Consider the kinematic model (13a) (13b). Assume there exists a positive σ satisfying $F^T F \leq \sigma^2$, $\sigma > 0$ due to the boundedness of d_V and d_θ . Choose the controller

$$\begin{bmatrix} \alpha_V^* \\ \alpha_\eta^* \end{bmatrix} = -(k_1\mu_1 + \frac{h_1\dot{\tau}}{\tau}) \begin{bmatrix} R_e \\ Rq_e \end{bmatrix} - G + M \begin{bmatrix} V_d \\ \eta_d \end{bmatrix}, \quad (22a)$$

$$\begin{bmatrix} V_s^* \\ \eta_s^* \end{bmatrix} = \begin{cases} M^{-1} \begin{bmatrix} \alpha_V^* & \alpha_\eta^* \end{bmatrix}^T, & t \in [0, t_f) \\ f_M(\begin{bmatrix} \alpha_V^* & \alpha_\eta^* \end{bmatrix}), & t \in [t_f, \infty) \end{cases} \quad (22b)$$

$$\begin{bmatrix} u_V \\ u_\theta \end{bmatrix} = B^{-1} \left\{ -((k_2 + \lambda_2)\mu_2 + \frac{h_2\dot{\tau}}{\tau}) \begin{bmatrix} e_V \\ e_\eta \end{bmatrix} - \begin{bmatrix} \dot{V}_s^* \\ \dot{\eta}_s^* \end{bmatrix} - H \right\} \quad (22c)$$

where $k_1 > 0$, $k_2 > 0$, $\lambda_2 > 0$ and the function

$$f_M(\begin{bmatrix} \alpha_V^* & \alpha_\eta^* \end{bmatrix}) = \begin{bmatrix} \|\begin{bmatrix} \alpha_V^* & \alpha_\eta^* \end{bmatrix}\| \\ \text{atan}(-\alpha_V^*/\alpha_\eta^*) \end{bmatrix}.$$

Define the tracking errors $e_V = V_s - V_s^*$, $e_\eta = \eta_s - \eta_s^*$. Consequently, the closed-loop system is prescribed-time stable, which means, (R_e, q_e, e_V, e_η) converges to the origin before $t = t_f$. Furthermore, one obtains

- (i) when $R_f = 0$, the choices of $\mu_1(t)$ and $\mu_2(t)$ should satisfy $\lim_{t \rightarrow t_f} (t_f - t)\mu_1\mu_2 = \infty$;
- (ii) when $R_f > 0$, the formation gets maintained in (R_f, q_f) through $V_{df} = 0$, $\dot{\eta}_d = 0$ and $\dot{V}_d = 0$ for $t \geq t_f$.

Proof. The proof is divided into four step:

Step 1. Prescribed-time convergences of R_e and q_e under V_s^* and η_s^* in (22b) before $t = t_f$.

With the controller (22b), the error dynamics is obtained as

$$\begin{bmatrix} \dot{R}_e \\ \dot{q}_e \end{bmatrix} = -(k_1\mu_1 + \frac{h_1\dot{\tau}}{\tau}) \begin{bmatrix} R_e \\ q_e \end{bmatrix}. \quad (23)$$

Consider the Lyapunov candidate $V_1(r) = x_1^T x_1$ and $W_1(r) = \mu_1^2 x_1^T x_1 = \omega_1^T \omega_1$ with $x_1 = \begin{bmatrix} R_e & q_e \end{bmatrix}^T$ and $\omega_1 = \mu_1 \begin{bmatrix} R_e & q_e \end{bmatrix}^T$. The derivative of $W_1(r)$ along (23) is

$$\begin{aligned} \dot{W}_1(t) &= 2\omega_1^T [\dot{\mu}_1 x_1 - (k_1\mu_1 + \dot{\tau}/\tau)\mu_1 \omega_1] \\ &= 2\omega_1^T [h_1(\dot{\tau}/\tau)\omega_1 - (k_1\mu_1 + h_1\dot{\tau}/\tau)\omega_1] \\ &\leq -2k_1\mu_1 W_1. \end{aligned} \quad (24)$$

Solving this differential inequality and invoking the fact $\int_0^t \mu_1(v)dv = -\phi_1(t)$ give $\mu_1^2(t)V_1(t) < \exp^{2k_1\phi_1}W_1(0)$ which yields

$$\left\| \begin{bmatrix} R_e \\ q_e \end{bmatrix} \right\| \leq \frac{1}{\mu_1(t)} \exp^{k_1\phi_1} (R_e^2(0) + q_e^2(0)). \quad (25)$$

where $\phi_1(t) = \frac{t_f}{h_1-1}(1 - \mu_1^{(h_1-1)/h_1})$. Thus, the origin of system (23) is globally prescribed-time stable within the prescribed time t_f .

Step 2. Prescribed-time convergences of V_s to V_s^* and η_s to η_s^* under the proposed u_V and u_θ in (22c) before $t = t_f$.

With the controller (22c), the dynamic model of e_V , e_η is obtained as

$$\begin{bmatrix} \dot{e}_V \\ \dot{e}_\eta \end{bmatrix} = -((k_2 + \lambda_2)\mu_2 + \frac{h_2\dot{\tau}}{\tau}) \begin{bmatrix} e_V \\ e_\eta \end{bmatrix} + F. \quad (26)$$

Consider the Lyapunov candidate $V_2(t) = x_2^T x_2$ and $W_2(t) = \mu_2^2 x_2^T x_2 = \omega_2^T \omega_2$ with $x_2 = [e_V \ e_\eta]^T$ and $\omega_2 = \mu_2 [e_V \ e_\eta]^T$. By applying Young's inequality with $\lambda_2 > 0$, one obtains $\omega_2^T \mu_2 F \leq \lambda_2 \mu_2 \omega_2^T \omega_2 + \mu_2 F^T F / (4\lambda_2)$. In this way, the derivative of $W_2(t)$ with respect to the variable t yields

$$\begin{aligned} \dot{W}_2(t) &= 2\omega_2^T [\dot{\mu}_2 x_2 - ((k_2 + \lambda_2)\mu_2 + h_2\dot{\tau}/\tau)\omega_2 + \mu_2 F] \\ &\leq -2k_2\mu_2 W_2 + \mu_2 F^T F / (2\lambda_2). \end{aligned} \quad (27)$$

In view of $F^T F \leq \sigma^2$ and invoking Lemma 1 in [13], it is direct to deduce $\mu_2^2(t)V_2(t) < (\exp^{2k_2\phi_2}W_2(0) + \sigma^2/(4k_2\lambda_2))$ which yields

$$\left\| \begin{bmatrix} e_V \\ e_\eta \end{bmatrix} \right\| \leq \frac{1}{\mu_2} \left(\exp^{k_2\phi_2} (e_V^2(0) + e_\eta^2(0)) + \frac{\sigma}{2\sqrt{k_2\lambda_2}} \right) \quad (28)$$

where $\phi_2(t) = \frac{t_f}{h_2-1}(1 - \mu_2^{(h_2-1)/h_2})$. Thus, it follows the prescribed-time stability of (e_V, e_η) .

Step 3: Prescribed-time convergence of the cascaded system.

Combining the two system models into a cascaded form, we obtain

$$\begin{bmatrix} \dot{R}_e \\ \dot{q}_e \end{bmatrix} = -(k_1\mu_1 + \frac{h_1\dot{\tau}}{\tau}) \begin{bmatrix} R_e \\ q_e \end{bmatrix} + \bar{M} \begin{bmatrix} e_V \\ e_\eta \end{bmatrix}, \quad (29a)$$

$$\begin{bmatrix} \dot{e}_V \\ \dot{e}_\eta \end{bmatrix} = -((k_2 + \lambda_2)\mu_2 + \frac{h_2\dot{\tau}}{\tau}) \begin{bmatrix} e_V \\ e_\eta \end{bmatrix} + F. \quad (29b)$$

- (i) Under the case $R_f > 0$, it is obvious that $\|\bar{M}\|$ is bounded. In addition, $\alpha_{13}(\tau) = 2k_1\mu_1^3$, $\alpha_{14}(\tau) = 2\mu_1^2$, $\alpha_{15}(\tau) = k_1\mu_1$; $\alpha_{23}(\tau) = 2k_2\mu_2^3$, $\alpha_{24}(\tau) = 2\mu_2^2$,

$\alpha_{25}(\tau) = k_2\mu_2$. Invoking the proposed Theorem 2, the cascaded system is globally prescribed-time stable in the sense that the reference trajectory gets tracked before t_f ;

- (ii) Under the case $R_f = 0$, it is obvious that $\|\bar{M}\|$ is related to $1/(t_f - t)$ such that $\alpha_{16}(\tau) = \mu_1^2/(t_f - t)$. Invoking the proposed Theorem 2, the cascaded system is globally prescribed-time stable if only $\lim_{t \rightarrow t_f} \frac{1/(t_f - t)}{\mu_1\mu_2} = 0$.

Step 4: Formation keeping over $[t_f, \infty)$ when $R_f > 0$.

When $t \in [t_f, \infty)$, $\mu_1 = \mu_2 = 1$, $\dot{\tau} = 0$ such that the cascaded system is rewritten into

$$\begin{bmatrix} \dot{R}_e \\ \dot{q}_e \end{bmatrix} = -k_1 \begin{bmatrix} R_e \\ q_e \end{bmatrix} + \bar{M}_m \begin{bmatrix} e_V \\ e_\eta \end{bmatrix}, \quad (30a)$$

$$\begin{bmatrix} \dot{e}_V \\ \dot{e}_\eta \end{bmatrix} = -(k_2 + \lambda_2) \begin{bmatrix} e_V \\ e_\eta \end{bmatrix} + F \quad (30b)$$

where $V_d(t) = 0$, $\eta_d(t) = 0$, $t \geq t_f$ and $\bar{M}_m = \text{diag}(1, 1/R)M(R, \eta_s, e_\eta, V_s)$. Define the Lyapunov candidate $V = x_1^T x_1 + x_2^T x_2$ whose time derivative yields

$$\dot{V} \leq -(2k_1 - \|\bar{M}_m\|)x_1^T x_1 - (2k_2 - \|\bar{M}_m\|)x_2^T x_2 \quad (31)$$

where $k_1, k_2 > 0.5\|\bar{M}_m\|$. The corresponding stabilization is obvious established according to the above proof. \square

Remark 6. It is obvious that the larger k_i , h_i ($i = 1, 2$) are, the faster R_e , q_e converge. Invoking Remark 4, it is better to design $k_2\mu_2 > k_1\mu_1$ to make the states of different subsystems converge in a reasonable order. In addition, the high-order scaling of state by a function of time in [13] requires the parameter h to be positive integers greater than 1. Our results do not require such limitations.

4. Extensions to simultaneous tracking/formation of multi-vehicles

For the multi-agent tracking/formation scenario, a distinguishing requirement is the simultaneous arrival. Suppose that n vehicles, M_1, \dots, M_n , participates in a tracking/formation with respect to a single target. In the following, the variable X_i , $1 \leq i \leq n$ stands for the corresponding X of the i -th vehicle. With the above design and analysis, each vehicle realizes the prescribed-time stabilization, that is, it realizes the tracking of R_i to $R_{d,i}$ and q_i to $q_{d,i}$ before the terminal time $t_{f,i}$.

According to the proposed reference relative tracking trajectory theorem in Section II.A, for the simultaneous

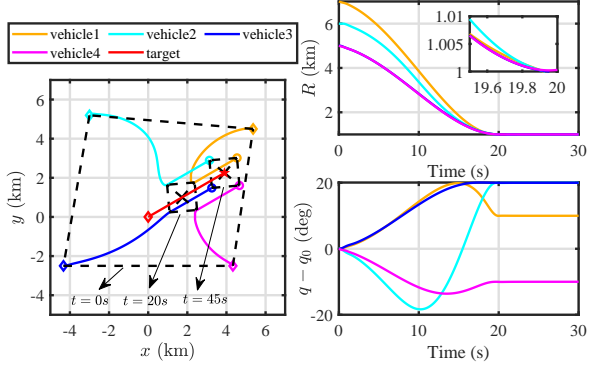


Figure 2: Trajectories of four vehicles

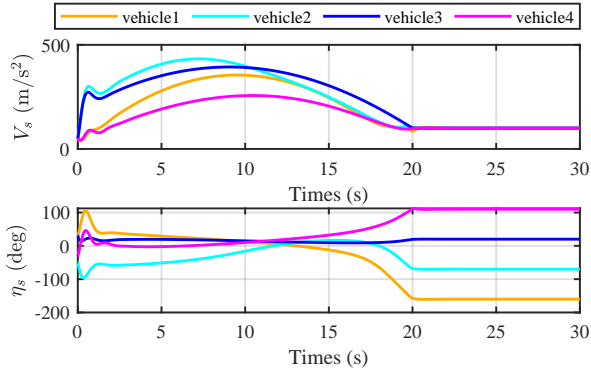


Figure 3: States of four vehicles

tracking/formation with $t_{f,i} = T_d$, the sufficient condition is $\int_0^{T_d} V_{d,i}(t)dt = S_{d,i}$, $i = 1, \dots, n$.

Assume a centralized coordination strategy exists between vehicles and the desired terminal time can be determined at the initial time. Thus, it is a direct solution to allocate the velocity reasonably to obtain simultaneous arrival. Below is an adjustment strategy which can achieve the smooth arrival to the terminal situation.

Construct a m -order polynomial function to describe the law of $V_{d,i}(t)$

$$V_{d,i}(t) = I_1 t^m + I_2 t^{m-1} + \dots + I_m t + I_{m+1} \quad (32)$$

which satisfies $m + 1$ equality constraints, including the following 3 necessary conditions

$$V_{d,i}(0) = V_{d0,i}, V_{d,i}(T_d) = V_{df,i}, \int_0^{T_d} V_{d,i}(\tau)d\tau = S_{d,i}.$$

5. Numerical examples

Suppose that four vehicles track a single target with the initial and terminal condition shown in Table 1. Each vehicle has the same initial velocity, 50 m/s.

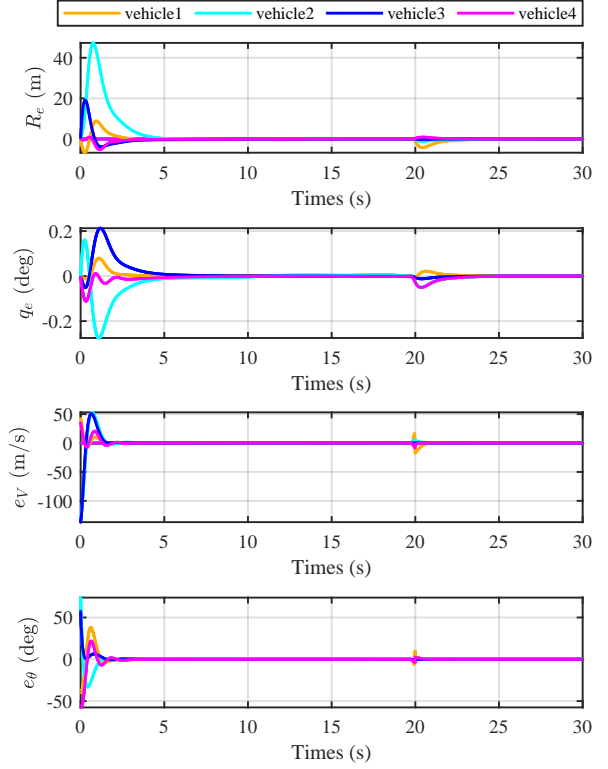


Figure 4: Tracking errors of four vehicles

For a target moving at a speed of $V_t = 100\text{m/s}$ in a 45-degree direction, the scenario at $T_d = t_{f,i} = 20\text{s}$ expects the four vehicles to be at a 90-degree angle to each other and a distance of 1000m from the target, meanwhile, it requires $V_{df,i} = 0\text{m/s}$ for the gentle transition to the phase of formation keeping $t > T_d$.

In accordance with (32), use a third-order polynomial for velocity planning. The function $\tau(t, t_f)$ is chosen in form of $\tau(t, t_f) = 1 + \ln(\frac{t_f}{t_f-t})$. The control parameters are as follows: $N_1 = 6$, $N_2 = 10$, $k_1 = 1$, $k_2 = 2$, $h_1 = 1$, $h_2 = 2$ and $\lambda_2 = 1$. The corresponding results for Case 2 can be found in Fig. 2-5. From the curves of R_i and q_i in Fig. 2, the simultaneous formation and formation

Table 1: Scenarios for simultaneous formation.

	Initial condition			Terminal condition	
	Distance R_0	LOS q_0	Path angle θ_0	Distance R_f	LOS q_f
Vehicle 1	7000 m	220 deg	190 deg	1000 m	230 deg
Vehicle 2	6000 m	-60 deg	-10 deg	1000 m	-40 deg
Vehicle 3	5000 m	30 deg	0 deg	1000 m	50 deg
Vehicle 4	5000 m	150 deg	180 deg	1000 m	140 deg

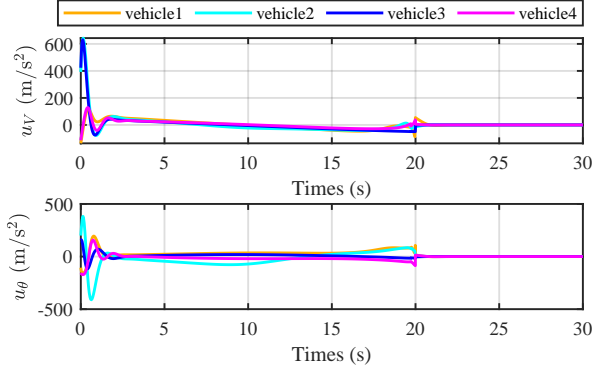


Figure 5: Control input of four vehicles

keeping are obvious achieved at T_d , and the transmission process to formation keeping is smooth due to the small value of the desired relative velocity $V_{df,i}$. The prescribed-time convergence of tracking errors can be obtained in Fig. 4. It is observed from Fig. 3 that the changes of both velocities and angles are slow towards the prescribed time T_d , which promotes the limited amount of control input near the time T_d as shown in Fig. 5. After the prescribed time T_d , the task becomes formation keeping relative to the target. The controller switching brings the controller mutation at time T_d in Fig. 5. As shown in the short period after T_d in Fig. 4, there is a regulation stage for the angle $\eta_{s,i}$ such that the speed of each vehicle gets to be parallel to that of the target.

It is worth emphasizing that the realization of simultaneous tracking and formation is completely dependent on the proposed space-and-time-synchronized strategy.

6. Conclusion

In this paper, we presented a space-and-time-synchronized control method for simultaneous tracking/formation. The resultant control is able to achieve the predetermined state at the prescribed terminal time with a fixed relative space trajectory independent of time. As a result, simultaneous tracking/formation of multiple vehicles can be directly implemented. Extending this method to the simultaneous tracking/formation with no predetermined terminal time under communication topologies is an interesting topic for future research.

A. Proof of Theorem 1

Step 1. Prescribed-distance stability before $r_d = r_f$.

Similar to the prescribed-time design philosophy in [23], we choose the controller (6) as a prescribed-distance controller by treating $r_f - r_d$ as a measure of the remaining distance to go. Substitution of (6) into (5) leads to second-order differential equation

$$\frac{d^2 q_d}{dr_d^2} + \frac{k_{d2}}{r_f - r_d} \frac{dq_d}{dr_d} + \frac{k_{d1}}{(r_f - r_d)^2} (q_d - q_f) = 0. \quad (33)$$

This is a kind of second-order Cauchy equation. Here, we introduce a scaling transformation $\zeta = \ln(r_f - r_d)$ with which the differential equation is transformed into

$$\frac{d^2 q_d}{d\zeta^2} - (k_{d2} + 1) \frac{dq_d}{d\zeta} + k_{d1} (q_d - q_f) = 0. \quad (34)$$

The corresponding characteristic equation is obtained by letting $q_d - q_f = e^{\lambda\zeta}$ as $\lambda^2 - (k_{d2} + 1)\lambda + k_{d1} = 0$ whose discriminant is $\Delta = (k_{d2} + 1)^2 - 4k_{d1}$. In order to obtain an elegant description of the solution, we make $\lambda_1 = N_1 \in \mathcal{N}_+$, $\lambda_2 = N_2 \in \mathcal{N}_+$, $N_1 < N_2$ which brings about $k_{d1} = N_1 N_2$, $k_{d2} = N_1 + N_2 - 1$, and the discriminant $\Delta > 0$. Hence, with the initial condition $q_d(0) = q_0$ and $\tan(\eta_d(0)) = \tan \eta_{d0}$, the solution of this Cauchy equation can be obtained

$$q_d(r_d) = C_1 (r_f - r_d)^{N_1} + C_2 (r_f - r_d)^{N_2} + q_f \quad (35)$$

where

$$C_1 = \frac{N_2(q_0 - q_f) + r_f \tan \eta_{d0} (R_0 - R_{f1})/R_0}{(N_2 - N_1)r_f^{N_1}},$$

$$C_2 = \frac{N_1(q_f - q_0) - r_f \tan \eta_{d0} (R_0 - R_{f1})/R_0}{(N_2 - N_1)r_f^{N_2}}.$$

Differentiating $q_d(r_d)$ with respect to r_d yields

$$\tan \eta_d = -\frac{R_d}{R_d - R_{f1}} \left[N_1 C_1 (r_f - r_d)^{N_1-1} + N_2 C_2 (r_f - r_d)^{N_2-1} \right]. \quad (36)$$

It is thus clear that, given the positive integers N_1, N_2 , as r_d approaching r_f , $q_d(r_d)$ and $\eta_d(r_d)$ converges to q_f and 0, respectively.

Step 2. Position maintaining after R_d approaching R_f .

Since $\eta_d(r_f) = 0$ in (36), $\eta_d(r_d) \equiv 0$ through $\dot{\eta}_d = 0$ for $r_d \geq r_f$. When $V_{df} = 0$ and $\dot{V}_d = 0$ for $r_d \geq r_f$, it is apparent $R_d \equiv R_f$ after R_d approaching R_f . Invoking $d^2 q_d / dr_d^2 = 0$ in (5), one obtains $q_d(r_d) \equiv 0$.

B. Proof of Theorem 2

We start from the simplified cascaded system with $n = 2$ subsystems. Evidently the prescribed-time stability of $x_2(t)$ in system Σ_2 can be obtained by taking

time derivative of $V_2(t, x_2)$

$$\begin{aligned} \dot{V}_2 &\leq -\alpha_{23}(\tau)\|x_2\|^2 + b_2(\alpha_{24}^2(\tau)/\alpha_{23}(\tau))\|\Delta_{x,2}\|^2 \\ &= -\delta_2\alpha_{23}\|x_2\|^2 \\ &\quad - \alpha_{23} \left[(1 - \delta_2)\|x_2\|^2 - b_2\|\Delta_{x,2}\|^2/\alpha_{25}^2 \right] \end{aligned} \quad (37)$$

with $\delta_2 \in (0, 1)$. Define the region $\Omega_{x_2}(r) = \{x_2 | \alpha_{25}^2\|x_2\|^2 \leq b_2\|\Delta_{x,2}\|^2/(1 - \delta_2)\}$ and we get $\Omega_{x_2}(t_f) = \lim_{t \rightarrow t_f} \Omega_{x_2}(t) = 0$, following from $\lim_{t \rightarrow t_f} \alpha_{25}(\tau) = \infty$. When x_2 is outside of $\Omega_{x_2}(r)$, the increasing property of $\alpha_{23}(\tau)$ will force x_2 to $\Omega_{x_2}(t)$; once x_2 is inside of $\Omega_{x_2}(t)$, x_2 will never escape $\Omega_{x_2}(t)$ and converge to 0 as t approaching t_f .

Then, the time derivative of $V_1(t, x_1)$ along Σ_1 becomes

$$\begin{aligned} \dot{V}_1 &\leq -\alpha_{13}\|x_1\|^2 + b_1(\alpha_{14}^2/\alpha_{13})\|\Delta_{x,1}\|^2 + \alpha_{16}c_{g,1}\|x_1\|\|x_2\| \\ &= -0.5\delta_1\alpha_{13}\|x_1\|^2 - \alpha_{13} \left[(1 - \delta_1)\|x_1\|^2 \right. \\ &\quad \left. - \gamma\alpha_{16}^2\|x_2\|^2/\alpha_{13}^2 - b_1\|\Delta_{x,1}\|^2/\alpha_{15}^2 \right] \end{aligned} \quad (38)$$

where $\gamma = 0.5c_{\theta}^2/\delta_1$. In view of the relationship among α_{13} , α_{16} and α_{25} , one obtains

$$\begin{aligned} \lim_{t \rightarrow t_f} \alpha_{16}^2\|x_2\|^2/\alpha_{13}^2 &= \alpha_{16}^2/(\alpha_{13}^2\alpha_{25}^2)\|\Delta_{x,2}\|^2 b_2/(1 - \delta_2) \\ &= 0. \end{aligned} \quad (39)$$

Invoking the boundedness of $\|\Delta_{x,1}\|^2$, the prescribed-time convergence of x_1 in system Σ_1 can be proved.

The prescribed-time convergence of cascaded system with $n = 2$ is thus concluded. From the prescribed-time stability of subsystems Σ_n and $\hat{\Sigma}_{n-1}$, the prescribed-time stability of Σ_{n-1} system is obtained; from the prescribed-time stability of subsystems Σ_{n-1} and $\hat{\Sigma}_{n-2}$, the prescribed-time stability of system Σ_{n-2} is obtained; and so on, the prescribed-time stability of Σ_1 system can be obtained. The proof is thus completed.

References

- [1] A. P. Aguiar, J. P. Hespanha, Trajectory-tracking and path-following of underactuated autonomous vehicles with parametric modeling uncertainty, *IEEE transactions on automatic control* 52 (8) (2007) 1362–1379.
- [2] B. Wang, H. Ashrafiuon, S. Nersesov, Leader–follower formation stabilization and tracking control for heterogeneous planar underactuated vehicle networks, *Systems & Control Letters* 156 (2021) 105008.
- [3] Y.-W. Wang, X.-K. Liu, J.-W. Xiao, Y. Shen, Output formation-containment of interacted heterogeneous linear systems by distributed hybrid active control, *Automatica* 93 (2018) 26–32.
- [4] X. Liu, S. S. Ge, C. Goh, Y. Li, Event-triggered coordination for formation tracking control in constrained space with limited communication, *IEEE transactions on cybernetics* 49 (3) (2018) 1000–1011.
- [5] J. Davila, Exact Tracking Using Backstepping Control Design and High-Order Sliding Modes, *IEEE Transactions on Automatic Control* 58 (8) (2013) 2077–2081.
- [6] A. Levant, Homogeneity approach to high-order sliding mode design, *Automatica* 41 (2005) 823 – 830.
- [7] S. Bhat, D. Bernstein, Geometric homogeneity with applications to finite-time stability, *Math. Control Signals Syst.* 17 (2005) 101 – 127.
- [8] Q. Hu, W. Chen, Y. Zhang, Concurrent Proximity Control of Servicing Spacecraft With an Uncontrolled Target, *IEEE/ASME Transactions on Mechatronics* 24 (6) (2019) 2815–2826.
- [9] B. Tian, Z. Zuo, X. Yan, H. Wang, A fixed-time output feedback control scheme for double integrator systems, *Automatica* 80 (2017) 17 – 24.
- [10] A. Polyakov, D. Efimov, W. Perruquetti, Finite-time and fixed-time stabilization: Implicit Lyapunov function approach, *Automatica* 51 (2015) 332 – 340.
- [11] Z. Zuo, Q.-L. Han, B. Ning, X. Ge, X.-M. Zhang, An Overview of Recent Advances in Fixed-Time Cooperative Control of Multi-agent Systems, *IEEE Transactions on Industrial Informatics* 14 (6) (2018) 2322–2334.
- [12] Y. Wang, Y. Song, D. J. Hill, M. Krstic, Prescribed-time consensus and containment control of networked multiagent systems, *IEEE transactions on cybernetics* 49 (4) (2018) 1138–1147.
- [13] Y. Song, Y. Wang, J. Holloway, M. Krstic, Time-varying feedback for regulation of normal-form nonlinear systems in prescribed finite time, *Automatica* 83 (2017) 243–251.
- [14] Y. Wang, Y. Song, Leader-following control of high-order multi-agent systems under directed graphs: Pre-specified finite time approach, *Automatica* 87 (2018) 113–120.
- [15] Y. Cao, W. Ren, Finite-time consensus for multi-agent networks with unknown inherent nonlinear dynamics, *Automatica* 50 (10) (2014) 2648–2656.
- [16] L. Zhao, Y. Jia, J. Yu, Adaptive finite-time bipartite consensus for second-order multi-agent systems with antagonistic interactions, *Systems & Control Letters* 102 (2017) 22–31.
- [17] X. Shao, Q. Hu, Y. Shi, Adaptive Pose Control for Spacecraft Proximity Operations With Prescribed Performance Under Spatial Motion Constraints, *IEEE Transactions on Control Systems Technology*.
- [18] J. Zhou, J. Yang, Distributed guidance law design for cooperative simultaneous attacks with multiple missiles, *Journal of Guidance, Control, and Dynamics* 39 (10) (2016) 2439–2447.
- [19] X. Chen, J. Wang, Optimal control based guidance law to control both impact time and impact angle, *Aerospace Science and Technology* 84 (2019) 454–463.
- [20] D. Li, H. Yu, K. P. Tee, Y. Wu, S. S. Ge, T. H. Lee, On Time-Synchronized Stability and Control, *IEEE Transactions on Systems, Man, and Cybernetics: Systems* (2021) 1–14.
- [21] D. Li, S. S. Ge, T. H. Lee, Fixed-Time-Synchronized Consensus Control of Multiagent Systems, *IEEE Transactions on Control of Network Systems* 8 (1) (2021) 89–98.
- [22] E. Panteley, A. Loria, Growth rate conditions for uniform asymptotic stability of cascaded time-varying systems, *Automatica* 37 (3) (2001) 453 – 460.
- [23] P. Wang, X. B. Zhang, S. S. Ge, Prescribed-time control with explicit reference governor for a class of constrained cascaded systems, *International Journal of Robust and Nonlinear Control* (2021) 1–16.